

# Pseudospectral vs Finite Difference Methods for Initial Value Problems with Discontinuous Coefficients

Erding Luo \*      Heinz-Otto Kreiss<sup>†</sup>

June 9, 1995

## Abstract

An initial value problem with piecewise constant coefficients is considered. The accuracies for both finite difference methods and the pseudospectral method are analyzed, and a modification of the initial value problem is suggested. The modified problem is shown to have the same temporal period as the original problem does, and a second order accuracy is obtained for the pseudospectral method at integral multiples of the temporal period.

## 1 Introduction

The pseudospectral method is very powerful for periodic initial value problems with constant coefficients. Well known results include its convergence at a spectral rate, [2, 3, 4, 8, 9]. This is largely because the eigenfunctions for the pseudospectral method are exactly those of fourier modes. Hence, the error for the pseudospectral method is not bigger than the truncated error of the initial value. For equations with jump coefficients, however, the pseudospectral method is far from being clear, even for one dimensional case, [1, 4, 5, 6, 7]. For such a problem, a large number of fourier eigenmodes to well represent all the eigenfunctions of the problem is needed in order to maintain a fast convergence rate, [3, 4].

The purpose of this paper is to compare the pseudospectral method with finite difference methods. For this, we will focus on an one dimensional periodic boundary wave equation, with a specific initial condition. The coefficient of the problem is assumed to be a piecewise constant function. We study the accuracies both for finite difference methods and the pseudospectral method using eigenfunction analysis. Our approach is to determine how many fourier eigenmodes are needed to well represent the initial condition with a given accuracy, and to analyze the accuracies of these eigenmodes. For finite difference methods, local truncation error analysis is used to obtain a global error estimate. For the pseudospectral method, the error estimate is generated by numerical computations. Since the coefficient is discontinuous, with an arbitrary discretization in the spatial domain, the accuracies of numerical methods may be affected by the values around the discontinuous positions. For

---

\*IMA, University of Minnesota, Mpls, MN 55455. Research supported by NSF through IMA.

<sup>†</sup>Department of Mathematics, University of California at Los Angeles, LA, CA90024.

the case in which the discontinuous points align with grid points, the harmonic values of the adjacent points are suggested for the coefficient at these discontinuous points. Under this construction, finite difference schemes give us an accuracy with order  $O(h\sqrt{h})$  in  $l_2$  norm and  $O(h)$  in  $l_\infty$  norm. In general, we do not know the exact locations of the discontinuous points. Both finite difference methods and the pseudospectral method give us an approximation with a shift. First order accuracy is always what we can expect, [1]. To improve this accuracy, we suggest a modified problem by truncating the fourier expansion of the inverse of the coefficient. This modified problem retains the same temporal period as the original one. It turns out that the pseudospectral method still has  $O(h)$  accuracy in  $l_\infty$  norm, but  $O(h\sqrt{h})$  in  $l_2$  norm. Moreover, at integral multiples of the temporal period, the pseudospectral method always has  $O(h^2)$  accuracy in  $l_\infty$  norm.

The rest of the paper is organized as follows: our model problem is presented in section 2. In section 3, Numerical schemes are introduced. The accuracies of both numerical methods are demonstrated in section 4 and some numerical results are presented in section 5.

## 2 Model Problem

Consider the following equation

$$\frac{\partial u(x, t)}{\partial t} = -a(x)\frac{\partial u(x, t)}{\partial x}, \quad x \in (-1, 1) \quad (2.1)$$

with periodic boundary condition, where the coefficient  $a(x)$  is also periodic with two discontinuous points at  $x = -1/2, 1/2$ , such that

$$a(x) = \begin{cases} 0.5, & x \in (-0.5, 0.5), \\ 1, & x \in [-1, 1]/[-0.5, 0.5]. \end{cases} \quad (2.2)$$

The initial condition takes the following form,

$$f(x) = \exp(-Cx^2), \quad x \in [-1, 1]. \quad (2.3)$$

### 2.1 Analytic Solution

Denote the  $k$ th ( $k \in Z$ ) eigenfunction of (2.1) by  $\phi_k$ , which satisfies the periodic boundary condition. Then,

$$-a(x)\frac{\partial \phi_k(x)}{\partial x} = \lambda \phi_k(x).$$

Thus,

$$\phi_k(x) = \exp(-\lambda \int_{-1}^x \frac{1}{a(\xi)} d\xi),$$

where

$$\lambda = 2\pi i \mu k, \quad \mu = \left( \int_{-1}^1 \frac{1}{a(\xi)} d\xi \right)^{-1} = \frac{1}{3}.$$

Let

$$\lambda_k = 2\pi ik, \quad k \in Z.$$

Then,  $\phi_k$  can be rewritten as

$$\phi_k(x) = \exp(-\lambda_k \mu \int_{-1}^x \frac{1}{a(\xi)} d\xi), \quad x \in [-1, 1]. \quad (2.4)$$

The sequence  $\{\phi_k(x)\}$  forms an orthogonal base with the weighing function  $\frac{1}{a(x)}$  in the domain  $[-1, 1]$ . The solution of (2.1) can thus be expanded in terms of the eigenfunctions as

$$u(x, t) \sim \sum_k c_k \exp(\lambda_k \mu (t - \int_{-1}^x \frac{1}{a(\xi)} d\xi)), \quad (2.5)$$

where  $c_k (k \in Z)$  is a constant that is determined by the initial condition (2.3).

*Remark.* Using the characteristic functions, it can be shown that the analytic solution of equation (2.1) will not be affected by the values of the coefficient  $a(x)$  at discontinuous points.

## 2.2 Expansion of Initial Condition

Denote the fourier eigenmodes by

$$\varphi_k(x) = \exp(-\lambda_k x), \quad k \in Z. \quad (2.6)$$

The initial condition (2.3) can also be expanded in terms of a certain number of the fourier eigenmodes (2.6) within endurance accuracy.

**Theorem 2.1** *Let function  $f$  be as in (2.3) with the parameter  $C = 60$ . Then, a few number of fourier eigenmodes are sufficient to well represent the initial condition with 1% accuracy. More precisely, let  $M = 26$ ,*

$$|f(x) - \frac{1}{3} \sum_{k \geq -M/2}^{k < M/2} c_k \varphi_k(\frac{2x}{3} + \frac{1}{2})| \leq \frac{1}{100}, \quad \forall x \in [-1, 1],$$

where

$$c_k = \int_{-1}^1 \frac{1}{a(x)} f(x) \bar{\phi}_k(x) dx, \quad (2.7)$$

and  $\phi_k(x)$  is as in (2.4).

*Proof.* Define an auxiliary 1-periodic function

$$g(y) = 3f(\frac{3}{2}y - \frac{3}{4}), \quad y \in [0, 1].$$

Then, its fourier series is as follows,

$$g(y) = \sum_{k \geq -M/2}^{k < M/2} G_k \exp(-\lambda_k y) + \Theta_M, \quad \forall y,$$

where

$$G_k = \int_0^1 g(y) \exp(\lambda_k y) dy = 3 \int_0^1 f\left(\frac{3}{2}y - \frac{3}{4}\right) \exp(\lambda_k y) dy,$$

and

$$\Theta_M(y) = \sum_{\substack{k \geq M/2 \\ k < -M/2}} G_k \exp(-\lambda_k y)$$

denotes the residual of the truncated fourier series for  $g(y)$ . Since  $\frac{1}{2} < |x| \leq 1$ , it follows  $f(x) \leq \delta$  for some negligibly small number  $\delta$ . From (2.7), it follows

$$\begin{aligned} c_k &= \int_{-1}^1 \frac{1}{a(x)} f(x) \exp(\lambda_k \mu \int_{-1}^x \frac{1}{a(\xi)} d\xi) dx \\ &= 2 \int_{-1/2}^{1/2} f(x) \exp(\lambda_k \mu (2x + \frac{3}{2})) dx + O(\delta) \\ &= 3 \int_{1/6}^{5/6} f\left(\frac{3}{2}y - \frac{3}{4}\right) \exp(\lambda_k y) dy + O(\delta) \\ &= \int_0^1 \frac{1}{\mu} f\left(\frac{3}{2}y - \frac{3}{4}\right) \exp(\lambda_k y) dy + O(\delta) \\ &= G_k + O(\delta). \end{aligned}$$

Therefore,

$$g(y) = \sum_{\substack{k < M/2 \\ k \geq -M/2}} c_k \exp(-\lambda_k y) + O(\delta M) + \Theta_M, \quad \forall y,$$

which implies,

$$f(x) = \frac{1}{3} \sum_{\substack{k < M/2 \\ k \geq -M/2}} c_k \exp(-\lambda_k \mu (2x + \frac{3}{2})) + O(\delta M) + \Theta_M, \quad \forall x \in [-3/4, 3/4].$$

Since  $g(y)$  is 1-periodic, for all  $y \in [0, 1]/(1/6, 5/6)$ ,

$$g(y) = O(\delta).$$

Equivalently, for  $x \in [-1, 1]/(-3/4, 3/4)$ ,

$$\frac{1}{3} \sum_{\substack{k < M/2 \\ k \geq -M/2}} c_k \exp(-\lambda_k \mu (2x + \frac{3}{2})) + O(\delta M) + \Theta_M = O(\delta).$$

Thus, for all  $x \in [-1, 1]$ ,

$$f(x) - \frac{1}{3} \sum_{\substack{k < M/2 \\ k \geq -M/2}} c_k \varphi_k\left(\frac{2x}{3} + \frac{1}{2}\right) = O(\delta M) + \Theta_M.$$

Because  $\delta$  is negligible, setting  $s = -2/3\lambda_k$  it follows from integration by parts that

$$\begin{aligned}
|G_k| &\leq \left| -\frac{4C}{s^2} \exp(-\lambda_k/2) \int_{-3/4}^{3/4} \exp(sx - Cx^2)(1 - 2Cx^2)dx \right| \\
&\leq \left| -\frac{8C^2}{s^3} \exp(-\lambda_k/2) \int_{-3/4}^{3/4} \exp(sx - Cx^2)x(3 - 2Cx^2)dx \right| \\
&\leq \left| \frac{8C^2}{s^4} \exp(-\lambda_k/2) \int_{-3/4}^{3/4} \exp(sx - Cx^2)(3 - 12Cx^2 + 4C^2x^4)dx \right| \\
&\leq \left| -\frac{16C^3}{s^6} \exp(-\lambda_k/2) \int_{-3/4}^{3/4} \exp(sx - Cx^2)(15 - 90Cx^2 + 60C^2x^4 - 8C^3x^6)dx \right| \\
&\leq \dots \\
&\leq \left| -\frac{64C^5}{s^{10}} \exp(-\lambda_k/2) \int_{-3/4}^{3/4} \exp(sx - Cx^2)(945 - 9450Cx^2 + 12600C^2x^4 \right. \\
&\quad \left. - 5040C^3x^6 + 720C^4x^8 - 32C^5x^{10})dx \right|.
\end{aligned}$$

We can thus establish

$$|G_k| \leq \frac{90720C^5}{s^{10}}. \quad (2.8)$$

Consequently,

$$\begin{aligned}
|\Theta_M| &\leq \sum_{k < -M/2}^{k \geq M/2} |G_k| \leq \sum_{k < -M/2}^{k \geq M/2} \frac{90720C^5}{s^{10}} \\
&\leq \frac{90720C^5 \times 3^{10}}{2^{10}\pi^{10}M^9}.
\end{aligned}$$

In order that

$$|\Theta_M| \leq \frac{1}{100},$$

it suffices to set  $M = 26$ . Therefore,

$$\left| f(x) - \frac{1}{3} \sum_{k \geq -M/2}^{k < M/2} c_k \varphi_k\left(\frac{2x}{3} + \frac{1}{2}\right) \right| \leq \frac{1}{100}, \quad \forall x \in [-1, 1].$$

■

In summary, for the given initial condition (2.3) with the parameter  $C = 60$ , the number  $M$  of fourier eigenmodes needed to well represent the initial condition (2.3) is 26. The accuracy of the approximation of (2.1) is 1%. Since  $\varphi_k(\frac{2}{3}x + \frac{1}{2})$  is orthogonal in  $[-\frac{3}{4}, \frac{3}{4}]$ , a sufficient number of fourier eigenmodes in the entire domain  $[-1, 1]$  is 32 in order to maintain the same accuracy.

### 2.3 Modified Problem

We modify equation (2.1) as follows

$$\frac{\partial v(x, t)}{\partial t} = -\frac{1}{b(x)} \frac{\partial v(x, t)}{\partial x}, \quad x \in (-1, 1), \quad (2.9)$$

where the coefficient  $b(x)$  is the truncated fourier series of  $\frac{1}{a(x)}$ . Note first the fourier expansion of  $\frac{1}{a(x)}$  is

$$\frac{1}{a(x)} \sim \sum_{\omega=-\infty}^{\infty} \hat{b}_{\omega} \exp(i\omega\pi(x+1)),$$

where  $\hat{b}_{\omega}$  is the fourier coefficient of  $\frac{1}{a(x)}$  with an order of  $O(\frac{1}{\omega})$  given by

$$\hat{b}_{\omega} = \begin{cases} -\frac{1}{i\omega\pi} \sin \frac{\omega\pi}{2}, & \omega \neq 0; \\ \int_{-1}^1 \frac{1}{a(x)} dx, & \omega = 0. \end{cases}$$

If we let

$$R_N(x) = \sum_{\omega < -N/2}^{\omega \geq N/2} \hat{b}_{\omega} \exp(i\omega\pi(x+1)),$$

then  $b(x)$  can be written as

$$b(x) = \frac{1}{a(x)} - R_N(x) = \sum_{\omega \geq -N/2}^{\omega < N/2} \hat{b}_{\omega} \exp(i\omega\pi(x+1)). \quad (2.10)$$

The eigenfunctions of (2.9) can be similarly analyzed as before. Denote the  $k$ th eigenfunction of (2.9) by  $\psi_k(x)$ . Then,

$$-\frac{1}{b(x)} \frac{\partial \psi_k(x)}{\partial x} = \lambda \psi_k(x).$$

We have

$$\psi_k(x) = \exp(-\lambda_k \mu \int_{-1}^x b(\xi) d\xi), \quad x \in [-1, 1]. \quad (2.11)$$

The sequence  $\{\psi_k(x)\}$  forms an orthogonal base with the weighing function  $b(x)$  in the domain  $[-1, 1]$ .

Subtracting (2.4) from (2.11),

$$\begin{aligned} \phi_k(x) - \psi_k(x) &= \phi_k(x) (1 - \exp(\lambda_k \mu \int_{-1}^x R_N(\xi) d\xi)) \\ &= \phi_k(x) (-\lambda_k \mu \int_{-1}^x R_N(\xi) d\xi) + O\left(\frac{k^2}{N^2}\right) = O\left(\frac{k}{N}\right). \end{aligned} \quad (2.12)$$

**Theorem 2.2** *Assume  $T$  is the temporal period of equation (2.1). Then, the difference between the solutions for equations (2.1) and (2.9) is of the following order,*

$$u(x, t) - v(x, t) = \begin{cases} O\left(\frac{1}{N}\right), & \text{for } t \neq kT, \quad k \in Z, \\ 0, & \text{for } \textit{otherwise}. \end{cases}$$

*Proof.* Denote the characteristic functions of (2.1) and (2.9) by  $X(t)$  and  $Y(t)$ , respectively. Then

$$\frac{dX}{dt} = -a(X),$$

$$\frac{dY}{dt} = -\frac{1}{b(Y)}.$$

By integration,

$$\int^Y b(\xi)d\xi = -t + C, \quad (2.13)$$

$$\int^X b(\xi)d\xi + \int^X R_N(\xi)d\xi = -t + C. \quad (2.14)$$

At  $t = 0$ ,  $X(0) = Y(0)$ . Subtract (2.13) from (2.14),

$$\begin{aligned} \int_Y^X b(\xi)d\xi &= \int^X b(\xi)d\xi - \int^Y b(\xi)d\xi \\ &= \int^{X(0)} R_N(\xi)d\xi - \int^X R_N(\xi)d\xi = -\int_{X(0)}^X R_N(\xi)d\xi. \end{aligned}$$

Since  $b(x)$  is a positive number,

$$b(\theta)(X - Y) = -\int_{X(0)}^X R_N(\xi)d\xi, \quad (2.15)$$

where  $\theta \in [X, Y]$ . When  $t \neq kT$ ,  $k \in Z$ , the right hand side of (2.15) is either  $O(h)$  or zero. Therefore, given an initial condition, the difference between the solutions for (2.1) and (2.9) is of an order at most equal to  $O(\frac{1}{N})$ .  $\blacksquare$

*Remark.* The modified problem (2.9) has the same temporal period as that of the original problem (2.1). If a same initial condition is used, the approximate solution of (2.1) by the pseudospectral method through the modified problem (2.9) has a second order accuracy when time  $t$  equals any integral multiple of the temporal period. (See discussion in Section 4.3.1)

### 3 Numerical Scheme

Divide the domain  $[-1, 1]$  with equal step size  $h$  by grid points  $\{x_j\}$ , and denote by  $u_j$  the approximation of the solution of equation (2.1) at  $x_j$  for  $j = 0, 1, \dots, N$ . Since the coefficient in the equation is strictly positive, finite difference methods and the pseudospectral method are stable, [7]. In this section, we add dissipations both to finite difference methods and to the pseudospectral method, in order to reduce the high frequency modes caused by the discontinuity of the coefficient.

#### 3.1 Finite Difference Methods

The discretized equation of (2.1) for the finite difference method is

$$\frac{du_j}{dt} = -a(x_j)Q_p u_j, \quad j = 0, 1, \dots, N - 1 \quad (3.16)$$

where  $Q_p$  is the centered difference operator that approximates  $\partial/\partial x$  with accuracy of order  $p$ . Thus,

$$Q_p = D_0 \sum_{\gamma=0}^{p/2-1} (-1)^\gamma \alpha_\gamma (h^2 D_+ D_-)^\gamma, \quad (3.17)$$

with the coefficients determined as follows,

$$\alpha_0 = 1, \quad (3.18)$$

$$\alpha_\gamma = \frac{\gamma}{4\gamma+2} \alpha_{\gamma-1}, \quad \gamma = 1, 2, \dots, p/2 - 2. \quad (3.19)$$

Assuming the 4-th order Runge-Kutta method with artificial dissipation is used for time discretization, we determine the approximation  $u_j^{n+1}$  at time level  $n+1$  from the previous approximation  $u_j^n$  in the following way,

$$\begin{aligned} u_j^{(n,1)} &= u_j^n, \\ u_j^{(n,2)} &= u_j^n - \frac{\Delta t}{2} a(x_j) Q_p u_j^{(n,1)}, \\ u_j^{(n,3)} &= u_j^n - \frac{\Delta t}{2} a(x_j) Q_p u_j^{(n,2)}, \\ u_j^{(n,4)} &= u_j^n - \Delta t a(x_j) Q_p u_j^{(n,3)}, \end{aligned}$$

and

$$\begin{aligned} u_j^{n+1} &= (1 + \gamma(-h)^{p+2} Q_{p+2}) u_j^n \\ &- \frac{\Delta t}{6} a(x_j) Q_p (u_j^{(n,1)} + 2u_j^{(n,2)} + 2u_j^{(n,3)} + u_j^{(n,4)}), \quad j = 0, 1, \dots, N-1. \end{aligned} \quad (3.20)$$

### 3.2 Pseudospectral Method

To apply the pseudospectral method to (2.1), we need first to determine a trigonometric polynomial in such a way that equation (2.1) holds true at all the grid points. Let  $U$  denote the vector with components  $u_j, j = 0, \dots, N-1$ . Then, under the pseudospectral method

$$\frac{dU}{dt} = ASU. \quad (3.21)$$

Here  $S$  presents the standard FFT operator. It is a  $N \times N$  matrix representing the discrete form of the differential operator  $\partial/\partial x$ .  $A$  is a diagonal matrix with entry  $a(x_j), j = 0, \dots, N-1$ . If the 4-th order Runge-Kutta method is used for time discretization with artificial dissipation, then the approximation  $U^{n+1}$  at time level  $n+1$  is determined from the approximation  $U^n$  at time level  $n$  as follows,

$$\begin{aligned} U^{(n,1)} &= U^n, \\ U^{(n,2)} &= U^n + \frac{\Delta t}{2} ASU^{(n,1)}, \\ U^{(n,3)} &= U^n + \frac{\Delta t}{2} ASU^{(n,2)}, \\ U^{(n,4)} &= U^n + \Delta t ASU^{(n,3)}, \end{aligned}$$



and

$$\begin{aligned} U^{n+1} &= \left(1 + \frac{\gamma h^{10}}{\pi^9} Q_{10}\right) U^n \\ &+ \frac{\Delta t}{6} AS(U^{(n,1)} + 2U^{(n,2)} + 2U^{(n,3)} + U^{(n,4)}). \end{aligned} \quad (3.22)$$

## 4 Accuracy Analysis

### 4.1 Truncation Error for Finite Difference

In this section, we analyze the local truncation error of the eigenfunction for the 2nd order finite difference method. We first establish

**Theorem 4.1** *Consider (2.1) with coefficient (2.2) and a partition of  $[-1, 1]$  with equal step  $h = \frac{2}{N}$  by grid points  $x_j = \frac{2j}{N} - 1$ ,  $j = 0, \dots, N$ . Assume the two discontinuous points  $-1/2$  and  $1/2$  align with two grid points, and at these two points, the values of the coefficient equal the harmonic values of two adjacent points, i.e.,  $a(-\frac{1}{2}) = a(\frac{1}{2}) = \frac{2}{3}$ . Then,*

$$a(x_j)(D_0\phi_k(x_j) - \frac{d\phi_k(x_j)}{dx}) = \begin{cases} O(\lambda_k^2 h), & x_j = -1/2, 1/2, \\ O(\lambda_k^3 h^2), & \text{otherwise,} \end{cases} \quad (4.23)$$

where  $\phi_k(x)$  is defined in (2.4).

*Proof.* Since

$$\phi_k(x) = \exp(-\lambda_k \mu \int_{-1}^x \frac{1}{a(\xi)} d\xi),$$

we have

$$\begin{aligned} \phi_k(x-h) &= \exp(-\lambda_k \mu \int_{-1}^{x-h} \frac{1}{a(\xi)} d\xi) = \phi_k(x) \exp(-\lambda_k \mu \int_x^{x-h} \frac{1}{a(\xi)} d\xi), \\ \phi_k(x+h) &= \exp(-\lambda_k \mu \int_{-1}^{x+h} \frac{1}{a(\xi)} d\xi) = \phi_k(x) \exp(-\lambda_k \mu \int_x^{x+h} \frac{1}{a(\xi)} d\xi). \end{aligned}$$

Simple calculation using Taylor expansion shows

$$2hD_0\phi_k(x_j) = 2h\phi_k(x_j)\left(-\frac{\lambda_k \mu}{a_j} + O(\lambda_k^3 h^2)\right) = 2h\phi_k(x_j)\left(-\frac{\lambda_k \mu}{a_j} + T_j\right)$$

for a continuous point  $x_j$  of  $a(x)$ , and for  $x_j = -\frac{1}{2}$  or  $\frac{1}{2}$ ,

$$2hD_0\phi_k(x_j) = 2h\phi_k(x_j)\left(-\frac{\lambda_k \mu}{a_j} + O(\lambda_k^2 h)\right) = 2h\phi_k(x_j)\left(\frac{-\lambda_k \mu}{a_j} + T_j\right),$$

where

$$T_j = \begin{cases} O(\lambda_k^2 h), & x_j = -1/2, 1/2, \\ O(\lambda_k^3 h^2), & \text{other } x_j. \end{cases}$$

■

*Remark.* Under the assumptions in Theorem 4.1, if the initial condition is chosen to be

$$u(x, 0) = \sum_{k \geq -M/2}^{k < M/2} c_k \phi_k(x), \quad \forall x \in [-1, 1],$$

then the analytic solution of (2.1) can be expressed in terms of the eigenfunctions as

$$u(x, t) = \sum_{k \geq -M/2}^{k \leq M/2-1} c_k \exp(\lambda_k \mu(t - \int_{-1}^x \frac{1}{a(\xi)} d\xi)). \quad (4.24)$$

We have

$$\begin{aligned} u(x_{j+1}, t) &= \sum_{k \geq -M/2}^{k < M/2} c_k \exp(\lambda_k \mu(t - \int_{-1}^{x_j} \frac{1}{a(\xi)} d\xi)) \exp(-\lambda_k \mu \int_{x_j}^{x_{j+1}} \frac{1}{a(\xi)} d\xi), \\ u(x_{j-1}, t) &= \sum_{k \geq -M/2}^{k < M/2} c_k \exp(\lambda_k \mu(t - \int_{-1}^{x_j} \frac{1}{a(\xi)} d\xi)) \exp(-\lambda_k \mu \int_{x_j}^{x_{j-1}} \frac{1}{a(\xi)} d\xi). \end{aligned}$$

Hence,

$$\begin{aligned} 2h D_0 u(x_j, t) &= u(x_{j+1}, t) - u(x_{j-1}, t) \\ &= 2h \sum_{k \geq -M/2}^{k < M/2} c_k \exp(\lambda_k \mu(t - \int_{-1}^{x_j} \frac{1}{a(\xi)} d\xi)) (-\frac{\lambda_k \mu}{a_j} + T_j), \end{aligned}$$

and

$$a(x_j)(D_0 u(x_j, t) - \frac{\partial u(x_j, t)}{\partial x}) = \sum_{k \geq -M/2}^{k < M/2} c_k \exp(\lambda_k \mu(t - \int_0^{x_j} \frac{1}{a(\xi)} d\xi)) a_j T_j.$$

Therefore

$$\begin{aligned} & \left| \sum_{k \geq -M/2}^{k < M/2} c_k \exp(\lambda_k \mu(t - \int_0^{x_j} \frac{1}{a(\xi)} d\xi)) a_j T_j \right| \\ &= \begin{cases} \sum_{k \geq -M/2}^{k < M/2} |c_k \lambda_k^2| O(h), & x_j = -1/2, 1/2 \\ \sum_{k \geq -M/2}^{k < M/2} |c_k \lambda_k^3| O(h^2), & \text{other } x_j. \end{cases} \end{aligned}$$

*Remark.* If the discontinuous points align with grid points, we may take the harmonic average values at those points. In so doing, the global truncation error can be improved to be  $O(h\sqrt{h})$  in  $l_2$  norm for the first few eigenfunctions with respect to the smallest eigenvalues. If the discontinuous points do not align with grid points, assigning the harmonic average values at those points is not possible. By taking the exact point values, the global truncation error we can obtain is in general  $O(h)$ . However, either one of them would give us an accuracy  $O(h)$  in  $l_\infty$  norm.

The order of numerical methods are usually determined by the number of eigenfunctions of the methods that can well approximate those of analytic ones. In our case, since we can explicitly write all the operators of the numerical methods, we are able to evaluate all the corresponding eigenpairs.

## 4.2 Eigenvalues

To compare the positive eigenvalues of the analytic problem, finite difference methods and the pseudospectral method, note first for the analytic eigenvalues,

$$\lambda_k = 2\pi k/3.$$

By taking grid points  $N = 32$  and  $N = 64$ , the eigenvalues are calculated and presented in Table 10 and Table 11. Throughout the rest of the paper, the notation “PS” stands for the pseudospectral method, “PS-mod” denotes the pseudospectral method with the coefficient  $b(x)$ . “FD2”, ..., “FD12” denotes 2nd to 12th order finite difference method, respectively. The values in the tables are divided by  $2\pi/3$ . The values at discontinuous points for coefficient  $a(x)$  are as in (5.27). From the comparison of eigenvalues, the pseudospectral method is not better than finite difference methods. And the higher order finite difference method is no longer superior to lower order ones either. It is evident that the lower number eigenvalues of PS-mod are much closer to the analytic ones than those of finite difference methods and PS. In the asymptotic region when the number of eigenvalues increases, there is virtually no difference among these methods. An implication is that when the number of grid points is not too big, PS-mod is presumably much superior to the other methods. However, as the number of the grid points increases, the accuracies of all the methods is seemingly the same.

*Remark.* In Table 10 and Table 11, we arrange the eigenvalues with respect to the frequencies of the corresponding eigenfunctions. In the columns corresponding to the analytic and pseudospectral methods, the number of the eigenvalues increases with the frequencies of the corresponding eigenfunctions. For the finite difference methods, the case is totally different. To illustrate this in more detail, consider an arbitrary fourier eigenmode, denoted by  $e^{i\omega x}$ . Then,

$$\frac{de^{i\omega x}}{dx} = i\omega e^{i\omega x},$$

and for the operator of the 2nd order finite difference method,

$$D_0 e^{i\omega x} = i \frac{\sin(\omega h)}{h} e^{i\omega x}.$$

When the frequency parameter  $\omega$  goes from 0 to  $\pi/h$ , the eigenvalues of the finite difference method behave exactly as a *sin* function, while the ones for the analytic and pseudospectral behave as a straight line.

## 4.3 Eigenvector

### 4.3.1 First Eigenvector

By numerical experiments for equation (2.1) with a discontinuous coefficient, either finite difference methods or the pseudospectral method would gives us an accuracy of  $O(h)$  in  $l_\infty$  norm. We demonstrate this by comparing the  $l_2$  and  $l_\infty$  norms of the difference of the first eigenfunction approximation for (2.1), using both 8th order finite difference method and the pseudospectral method in Table 1, Table 2 and Table 3.

norm	N=	16	32	64	128	256
2	FD8	0.1568	0.0778	0.0388	0.0194	0.0097
	PS	0.1246	0.0639	0.0323	0.0163	0.0082
$\infty$	FD8	0.2014	0.0992	0.0494	0.0247	0.0123
	PS	0.1367	0.0709	0.0361	0.0182	0.0091

Table 1: Accuracy of the first eigenfunction with (5.27)

norm	N=	16	32	64	128	256
2	FD8	0.0986	0.0507	0.0259	0.0131	0.0066
	PS	0.0570	0.0282	0.0141	0.0070	0.0035
$\infty$	FD8	0.1032	0.0531	0.0270	0.0137	0.0069
	PS	0.0868	0.0476	0.0248	0.0126	0.0064

Table 2: Accuracy of the first eigenfunction with (5.28)

The values of the coefficient at discontinuous points in Table 1, Table 2 and Table 3 are as in (5.26), (5.27) and (5.28) respectively (see section 5). In all these tables, we get  $O(h)$  accuracy in  $l_\infty$  norm. This is also true in  $l_2$  norm in Table 1 and Table 2. In Table 3 where we take the harmonic values at the discontinuous points and consider the pseudospectral method for the modified problem (2.9), the error in  $l_2$  norm is increased from  $O(h)$  to  $O(h\sqrt{h})$ . But, the pseudospectral method for the modified problem still gives us  $O(h)$  accuracy in  $l_\infty$  norm, due to the difference between the two analytic solutions in (2.1) and (2.9). If we only consider the accuracy of the approximation for (2.9) (instead of (2.1)), we can get  $O(h^2)$  both in  $l_2$  and  $l_\infty$  norms (see Table 4), which is determined by the construction of  $b(x)$  for  $a(x)$ .

norm	N=	16	32	64	128	256
2	FD8	0.0287	0.0089	0.0029	0.0010	3.4743E-4
	PS	0.0251	0.0089	0.0031	0.0011	3.9153E-4
	PS-mod	0.0144	0.0049	0.0017	5.9968E-4	2.1125E-4
$\infty$	FD8	0.0476	0.0227	0.0111	0.0055	0.0027
	PS	0.0498	0.0249	0.0124	0.0062	0.0031
	PS-mod	0.0273	0.0134	0.0067	0.0033	0.0017

Table 3: Accuracy of the first eigenfunction with (5.29)

norm	N=	16	32	64	128	256
2	PS-mod	0.0039	8.9968e-04	2.1335e-04	5.1556e-05	1.2613e-05
$\infty$	PS-mod	0.0042	0.0011	2.9377e-04	8.0042e-05	2.1793e-05

Table 4: Accuracy of the first eigenfunction for modified problem

### 4.3.2 Comparison of Other Eigenvectors

We now compare other eigenfunctions of finite difference methods and the pseudospectral method with the analytic ones. To do so, we take  $N$  equal to 64, and the values at discontinuous points to be (5.27). The  $k$ -th eigenfunction corresponds to the  $k$ -th eigenvalue, for  $k = -N/2, \dots, N/2 - 1$ . We define the  $k$ th eigenfunction of the numerical methods by checking if its corresponding eigenvalue is the closest one to the  $k$ th analytic eigenvalue. As we can see in Figures 1 to 4, the pseudospectral method gives a good representation of the analytic eigenfunctions for large eigenvalues.

## 5 Numerical Tests

In this section approximation for equation (2.1) is determined with the following initial value,

$$u(x, 0) = f(x) = \exp(-60x^2), \quad x \in [-1, 1]. \quad (5.25)$$

The errors in  $l_2$  and  $l_\infty$  norms of the pseudospectral method, 2nd to 12th order finite difference methods and Fourier Galerkin methods are compared after 3 analytic temporal period.

### 5.1 Jumps Not Aligning With Grid Points

When the jumps do not align with grid points, directly taking the values of the coefficient at the grid points usually gives an accuracy of  $O(h)$ . To see this, we assign values of the coefficient  $a(x)$  at discontinuous points to be as follows

$$a(x) = \begin{cases} 0.5, & x_j = -0.5 \\ 1, & x_j = 0.5. \end{cases} \quad (5.26)$$

The error of the approximation is presented in Table 5 and Fourier Galerkin method, denoted by ‘‘Galerkin’’, is also tested.

As shown in Table 5, the accuracy under these values of the coefficient is again  $O(h)$  for the finite difference methods and for the Fourier Galerkin method as well. For the pseudospectral method, the accuracy is almost  $O(h^2)$  which is certainly faster than other methods. The reason that the pseudospectral method works well here is because the exact speed happens to be at discontinuous points. Table 6 is obtained by adding dissipation to

norm	N=	32	64	128	256	512
2	FD2	0.4113	0.2493	0.1086	4.0140D-02	1.7064D-02
	FD4	0.2026	4.9328D-02	2.1710D-02	1.0524D-02	5.2225D-03
	FD6	9.1303D-02	1.1123D-02	5.7189D-03	2.8557D-03	1.4229D-03
	FD8	6.1094D-02	2.6830D-02	5.1059D-03	1.5851D-03	6.7531D-04
	FD10	0.1664	8.8547D-02	4.2848D-02	2.1040D-02	1.0482D-02
	FD12	6.1279D-02	2.0582D-02	1.1546D-02	5.8675D-03	2.9487D-03
	PS	9.5075D-03	1.6555D-03	5.2816D-04	1.3666D-04	1.4294D-05
	Galerkin	4.5006D-02	2.0152D-02	9.6680D-03	4.7562D-03	2.3633D-03
$\infty$	FD2	0.6023	0.4653	0.2240	6.2773D-02	2.0025D-02
	FD4	0.4028	9.3976D-02	3.1800D-02	1.1875D-02	5.5306D-03
	FD6	0.1585	1.4441D-02	6.6006D-03	3.2884D-03	1.6437D-03
	FD8	0.1421	3.8431D-02	8.8147D-03	2.3873D-03	9.3411D-04
	FD10	0.2166	9.6825D-02	5.2928D-02	2.4793D-02	1.1971D-02
	FD12	8.4801D-02	2.7116D-02	1.3545D-02	6.5436D-03	3.2070D-03
	PS	2.3121D-02	3.7157D-03	9.7142D-04	2.2080D-04	3.1296D-05
	Galerkin	9.5464D-02	4.3214D-02	2.0742D-02	1.016D-02	5.0481D-03

Table 5:  $\Delta t = 0.01h$ ,  $\gamma = 0$ , final time equals 9.

the schemes. Again, we get a similar phenomenon. In Table 7, we test the pseudospectral method by taking the following values for the coefficient at discontinuous points,

$$a(x) = \begin{cases} 1, & x_j = -0.5, \\ 1, & x_j = 0.5. \end{cases} \quad (5.27)$$

The usual accuracy  $O(h)$  for the pseudospectral method holds under these new values of the coefficient.

## 5.2 Jumps Aligning With Grid Points

Consider now the case where the discontinuous points align with grid points. For this case we are able to assign the values of  $a(x)$  at the discontinuous points to be the harmonic average. That is,

$$a(x) = \begin{cases} 2/3, & x = -0.5 \\ 2/3, & x = 0.5. \end{cases} \quad (5.28)$$

From Table 8, it's clear that the finite difference schemes has an accuracy of  $O(h^2)$ , and the accuracy for the pseudospectral method is even better. This happens partially because of the specific structure of the coefficient and initial condition. We should also note that some cancellations caused by the symmetric data occur here.

norm	N=	32	64	128	256	512
2	FD2	0.2473	0.1614	7.1518D-02	1.9820D-02	4.2894D-03
	FD4	0.1680	5.9871D-02	1.6548D-02	7.7677D-03	3.8663D-03
	FD6	0.1621	5.3195D-02	1.9151D-02	9.1902D-03	4.5534D-03
	FD8	0.1591	5.3081D-02	2.1103D-02	1.0171D-02	5.0415D-03
	FD10	0.1113	3.3988D-02	1.4989D-02	7.3021D-03	3.6280D-03
	FD12	0.1216	3.8618D-02	1.7053D-02	8.3027D-03	4.1246D-03
	PS	1.0558D-02	1.700D-03	3.9811D-04	1.1674D-04	4.1314D-05
$\infty$	FD2	0.5424	0.3355	0.1668	4.7679D-02	1.0050D-02
	FD4	0.3916	0.1415	4.1153D-02	1.6924D-02	8.2588D-03
	FD6	0.3557	0.1339	4.3324D-02	1.9688D-02	9.7204D-03
	FD8	0.3355	0.1365	4.6329D-02	2.1776D-02	1.0762D-02
	FD10	0.2236	8.0463D-02	3.2371D-02	1.5617D-02	7.7419D-03
	FD12	0.2463	9.1259D-02	3.6856D-02	1.7759D-02	8.8015D-03
	PS	2.2779D-02	3.9330D-03	8.6075D-04	2.4357D-04	8.6172D-05

Table 6:  $\Delta_t = 0.01h$ .  $\gamma$  is 0.001 for 2nd to 8th finite difference methods and pseudospectral method; Otherwise, it is 0.0001. Final time equals 9.

norm	N=	32	64	128	256	512
2	PS	0.2794	0.1448	7.2956D-02	3.6518D-02	1.8258D-02
$\infty$	PS	0.5618	0.3073	0.1552	7.7774D-02	3.8923D-02

Table 7:  $\Delta t = 0.01h$ ,  $\gamma = 0$ , final time equals 9.

### 5.3 Pseudospectral Method With Coefficient $b(x)$

Under the pseudospectral method with coefficient  $b(x)$ , the accuracy is improved from  $O(h)$  to  $O(h^2)$  as shown in Table 9. The approximation for (2.9) is calculated after 3 analytic temporal period. There is no difference between the analytic solutions of (2.1) and (2.9), since both have the same temporal period. We get an accuracy of  $O(h^2)$  that is entirely caused by the error of  $b(x)$  to  $a(x)$ .

**Acknowledgment.** We want to express our gratitude to Bengt Fornberg, whose short course given at IMA motivated our interest in finding an explanation for the problem considered in this paper.

## References

- [1] Brown, D.L., *A Note on the Numerical Solution of the Wave Equation With Piecewise Smooth Coefficients*, Mathematics of Computation, Vol. 42, No. 166, 1984, pp.369-391.

norm	N=	32	64	128	256	512
2	FD2	0.3868	0.2354	9.0539D-02	2.4744D-02	6.2381D-03
	FD4	0.1809	3.3606D-02	4.8228D-03	1.0429D-03	2.5622D-04
	FD6	8.8369D-02	5.2536D-03	6.7254D-04	1.6959D-04	4.2195D-05
	FD8	5.0305D-02	8.7695D-03	8.5339D-04	1.4887D-04	3.4517D-05
	FD10	6.6675D-02	1.9340D-02	4.5957D-03	1.1029D-03	2.7275D-04
	FD12	4.1083D-02	4.0960D-03	1.2958D-03	3.3263D-04	8.3718D-05
	PS	1.2908D-03	4.8477D-05	8.6714D-06	2.3430D-06	1.7069D-07
$\infty$	FD2	0.5379	0.4703	0.2349	6.4592D-02	1.5800D-02
	FD4	0.3014	7.6635D-02	1.0146D-02	1.3509D-03	2.6898D-04
	FD6	0.1601	1.5550D-02	1.2512D-03	2.3931D-04	5.6754D-05
	FD8	8.2814D-02	1.2156D-02	1.2001D-03	2.2163D-04	4.7924D-05
	FD10	1.0220D-01	2.7691D-02	5.3558D-03	1.2161D-03	2.9634D-04
	FD12	7.1897D-02	4.7769D-03	1.3942D-03	3.3311D-04	8.2901D-05
	PS	3.2908D-03	1.1687D-04	1.1099D-05	1.9323D-06	1.3546D-07

Table 8:  $\Delta t = 0.01h$ ,  $\gamma = 0$ , final time equals 9.

norm	N=	32	64	128	256	512
2	PS-mod	5.5522D-03	1.1314D-03	2.4839D-04	3.3473D-05	1.3400D-05
$\infty$	PS-mod	1.3857D-02	2.5183D-03	5.2898D-04	6.1899D-05	1.4724D-05

Table 9:  $\Delta t = 0.01h$ ,  $\gamma = 0$ , final time equals 9.

- [2] Canuto, C., Hussaini, M.Y., Quarteroni, A., and T.A. Zang, *Spectral Methods in Fluid Dynamics*, Springer-Verlag, 1988.
- [3] Gustafsson B., Kreiss, H-O, and Olinger, J. *Time Dependent Problems and Difference Methods*, 1994.
- [4] Kreiss, H. and Olinger J., *Methods for the Approximate Solution of Time Dependent Problems*, GARP, No. 10, 1973.
- [5] Fornberg, B. *The pseudospectral Methods: Accurate Representation of Interfaces in Elastic Wave Calculations*, Geophysics, Vol. 53, No. 5. (1988), pp. 625-637.
- [6] Fornberg, B. *The pseudospectral Method: Comparisons with Finite Differences for the Elastic Wave Equation*, Geophysics, Vol. 52, No. 4. (1987), pp. 483-501.
- [7] Fornberg, B. *On a Fourier Method For the Integration of Hyperbolic Equations*, SIAM J. Numer. Anal. Vol. 12, No. 4. (1975), pp. 509-528.



Analytic	PS	PS-mod	FD8	FD6	FD4	FD2
16.0000	22.2489	22.0982	0	0	0	0
15.0000	19.8029	19.5177	2.6527	2.2173	1.6759	1.0263
14.0000	17.4273	17.0101	4.9130	4.2152	3.2261	1.9592
13.0000	15.1367	14.6156	6.3823	5.5055	4.4369	2.7529
12.0000	13.0216	12.4933	12.9685	11.9026	4.7574	3.4542
11.0000	11.3617	11.0578	12.2427	11.2827	10.3159	3.4824
10.0000	10.2847	10.0401	11.1287	10.3139	9.8257	4.2914
9.0000	9.2229	9.0226	9.7456	9.0826	9.0452	6.7009
8.0000	8.1913	8.0094	8.2286	7.6978	8.0275	7.5323
7.0000	7.1625	7.0059	6.7813	6.3443	6.8479	7.2152
6.0000	6.1339	6.0038	5.9395	5.8380	5.6357	6.0120
5.0000	5.1102	5.0014	5.0706	4.9884	5.1309	5.1851
4.0000	4.0871	4.0006	4.0749	4.0077	3.9837	3.7644
3.0000	3.0644	3.0003	3.0634	3.0579	3.0198	2.8855
2.0000	2.0428	2.0001	2.0400	2.0317	2.0438	1.9834
1.0000	1.0213	1.0000	1.0213	1.0212	1.0208	0.9985

Table 10: Positive Eigenvalues for  $N = 32$ .

- [8] Fornberg, B. *A practical Guide to Pseudospectral methods*, Cambridge University Press, (to appear).
- [9] Gottlieb, D. and S.A. Orszag, *Numerical Analysis of Spectral Methods: Theory and Application*, SIAM, Philadelphia, Vol. 26, 1977.

Analytic	PS	PS-mod	FD8	FD6	FD4	FD2
32.0000	45.8393	45.7490	0	0	0	0
31.0000	43.1450	42.9778	2.6699	2.2155	1.6777	1.0144
30.0000	40.4984	40.2504	5.2430	4.3690	3.3225	2.0115
29.0000	37.8717	37.5410	7.6152	6.4005	4.8838	2.9412
28.0000	35.2647	34.8519	9.6960	8.2634	6.3602	3.8733
27.0000	32.6853	32.1943	11.4302	9.7182	7.6821	4.7500
26.0000	30.1493	29.5898	12.4716	10.7553	8.6475	5.5133
25.0000	27.6884	27.0828	12.7621	11.4436	9.4698	5.6393
24.0000	25.3807	24.7927	25.8441	11.8132	9.7214	6.3016
23.0000	23.4933	23.1295	26.2908	23.7289	10.2605	6.809
22.0000	22.3705	22.1027	25.1175	24.1053	10.4219	7.3052
21.0000	21.2986	21.0612	24.1367	23.1129	20.5742	7.4147
20.0000	20.2743	20.0370	22.9340	22.2738	20.8676	7.6005
19.0000	19.2494	19.0314	21.5465	21.2332	20.0913	14.2920
18.0000	18.2227	18.0229	20.0134	20.0172	19.4275	14.7205
17.0000	17.2066	17.0147	18.3740	18.6546	18.5950	15.2164
16.0000	16.1905	16.0122	16.6685	17.1769	17.6087	15.0297
15.0000	15.1732	15.0095	14.9462	15.6182	16.4865	13.7485
14.0000	14.1600	14.0061	13.3468	14.0214	15.2491	13.0957
13.0000	13.1467	13.0048	13.1206	12.4823	13.9209	12.3410
12.0000	12.1330	12.0038	11.8293	12.0224	12.5341	11.4935
11.0000	11.1211	11.0024	10.9809	11.0113	11.1498	10.5648
10.0000	10.1093	10.0017	10.0566	9.9927	10.0261	9.5718
9.0000	9.0973	9.0013	9.0729	8.9930	8.8724	8.5442
8.0000	8.0861	8.0008	8.0825	8.0018	7.8848	7.6175
7.0000	7.0749	7.0005	7.0722	7.0529	6.9595	6.9590
6.0000	6.0638	6.0003	6.0634	6.0450	6.0126	6.2809
5.0000	5.0531	5.0002	5.0522	5.0500	5.0407	4.8030
4.0000	4.0423	4.0001	4.0414	4.0364	4.0370	3.9267
3.0000	3.0316	3.0000	3.0320	3.0314	3.0279	3.0047
2.0000	2.0211	2.0000	2.0204	2.0188	2.0221	1.9960
1.0000	1.0105	1.0000	1.0105	1.0105	1.0105	1.0022

Table 11: Positive Eigenvalues for  $N = 64$

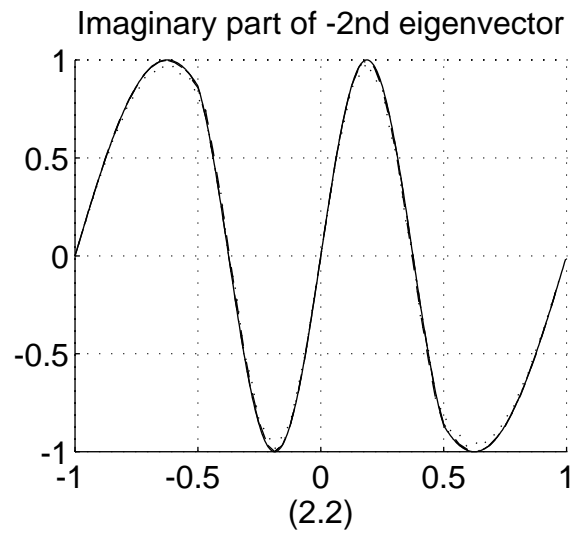
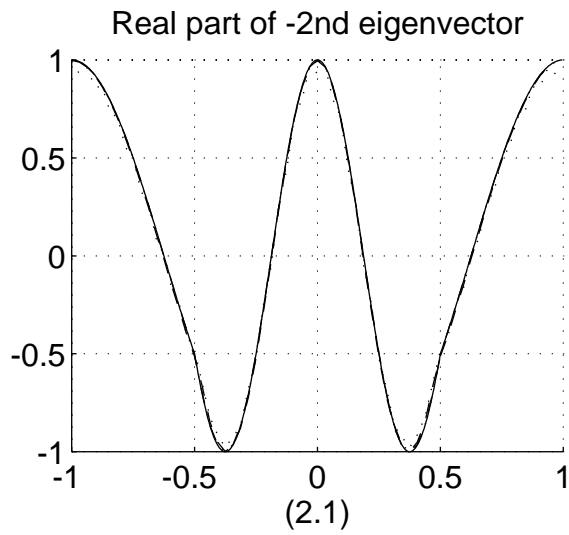
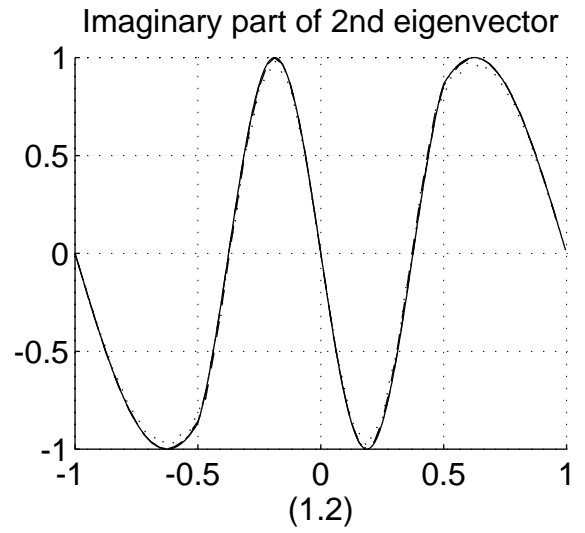
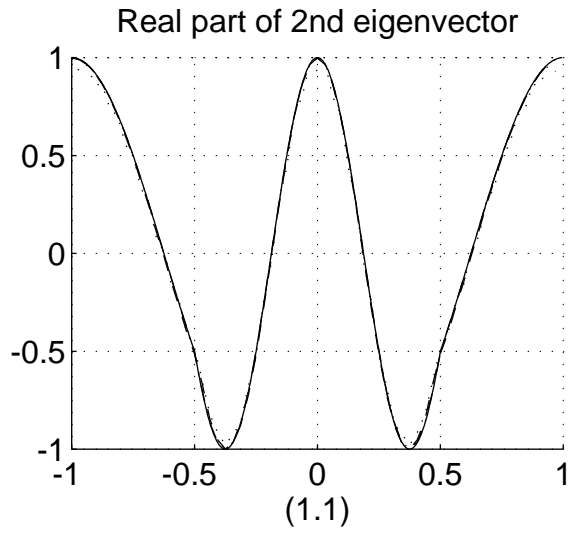


Figure 1: 2th and -2th eigenfunctions. Solid line represent the analytic eigenfunction; dot line for 8th order finite difference; dash line for the pseudospectral method and dashdot for the pseudospectral method with modified coefficient

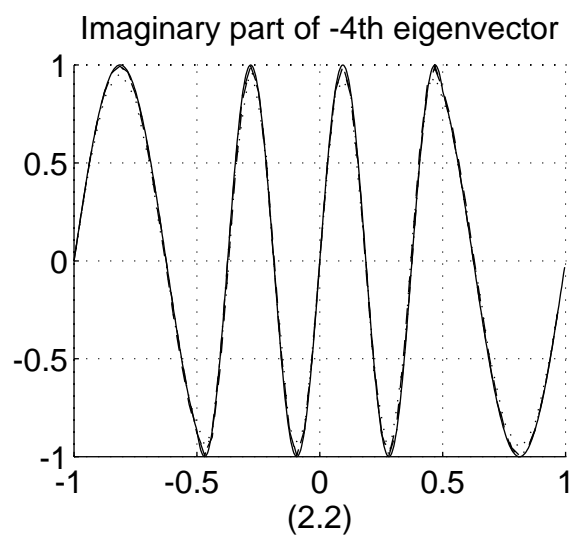
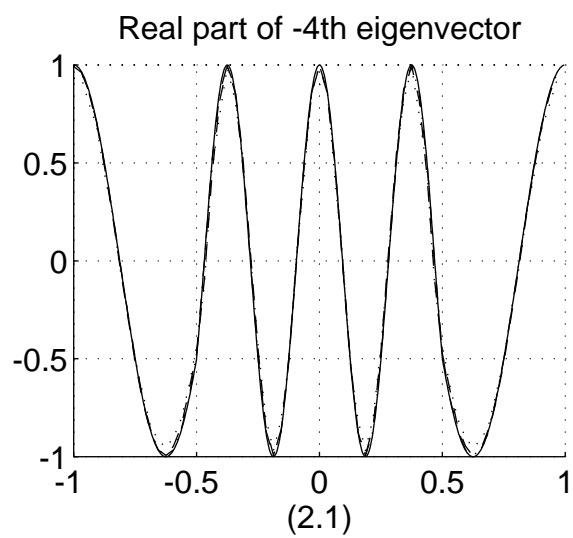
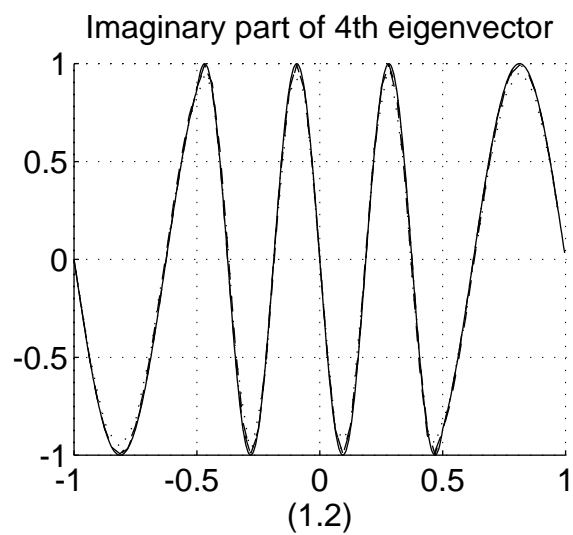
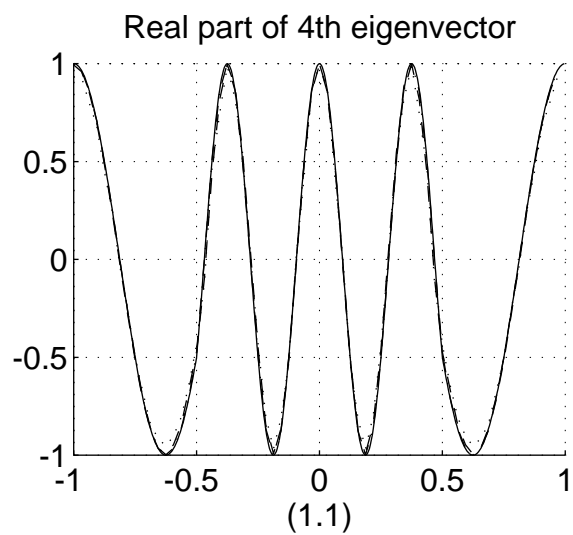


Figure 2: 4th and  $-4$ th eigenfunctions. Solid line represent the analytic eigenfunction; dot line for 8th order finite difference; dash line for the pseudospectral method and dashdot for the pseudospectral method with modified coefficient

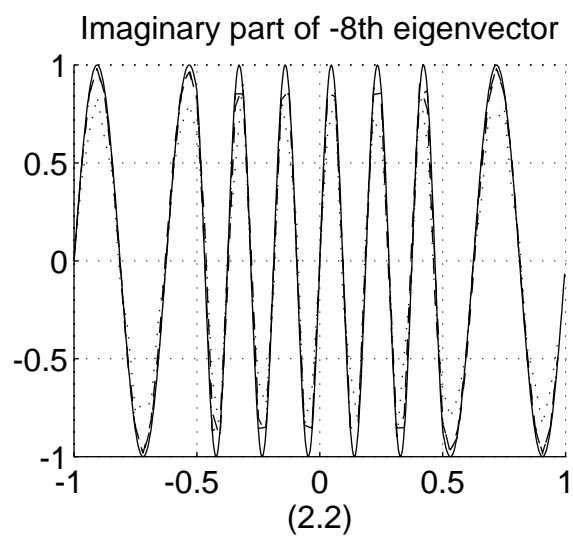
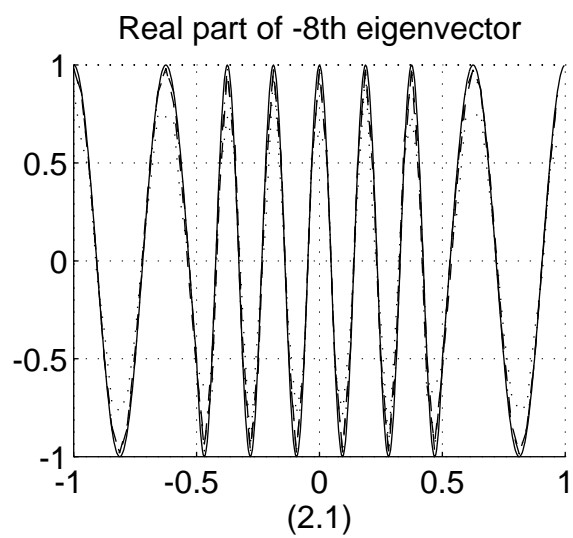
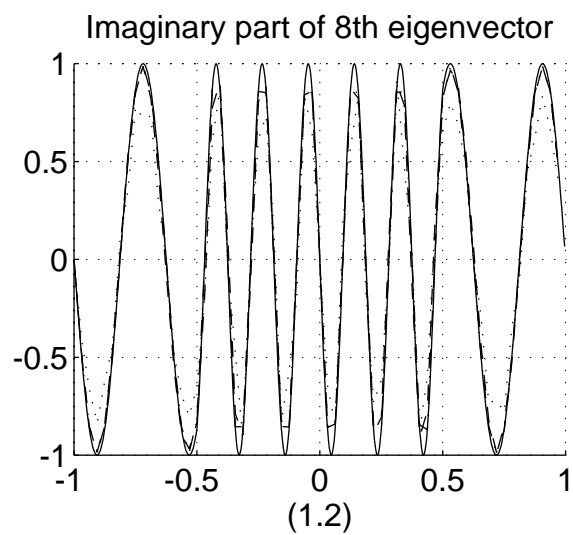
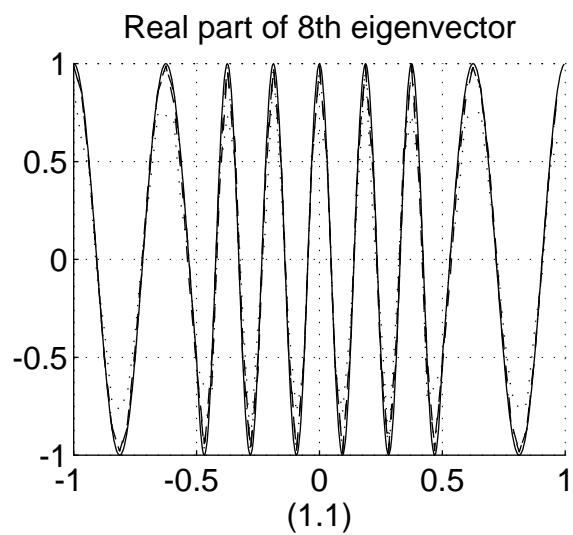


Figure 3: 8th and  $-8$ th eigenfunctions. Solid line represent the analytic eigenfunction; dot line for 8th order finite difference; dash line for the pseudospectral method and dashdot for the pseudospectral method with modified coefficient

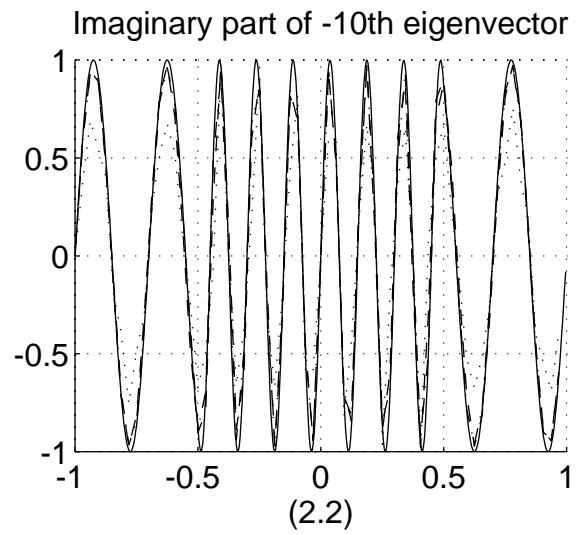
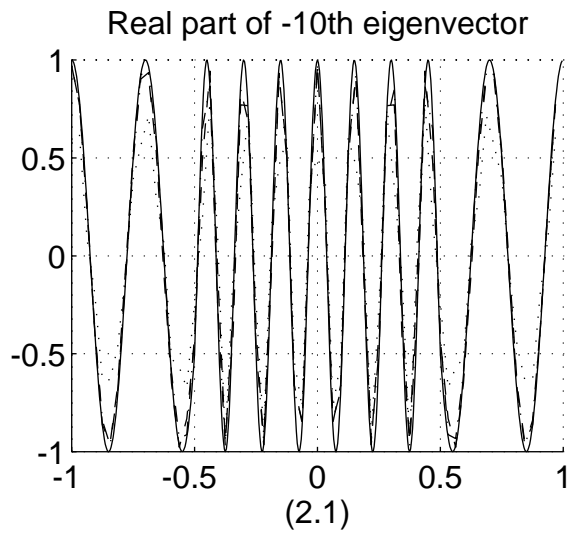
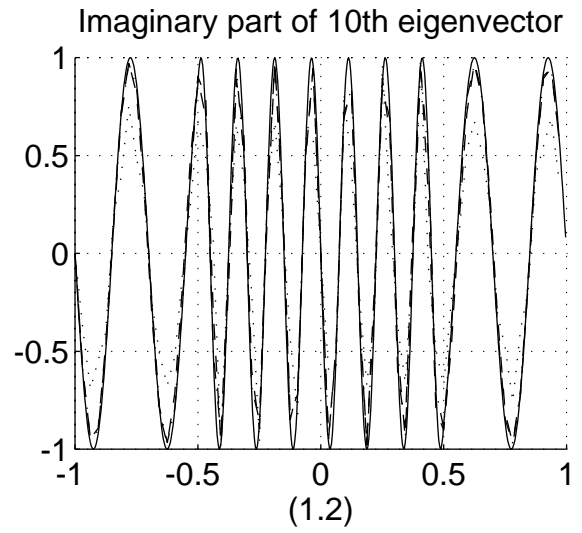
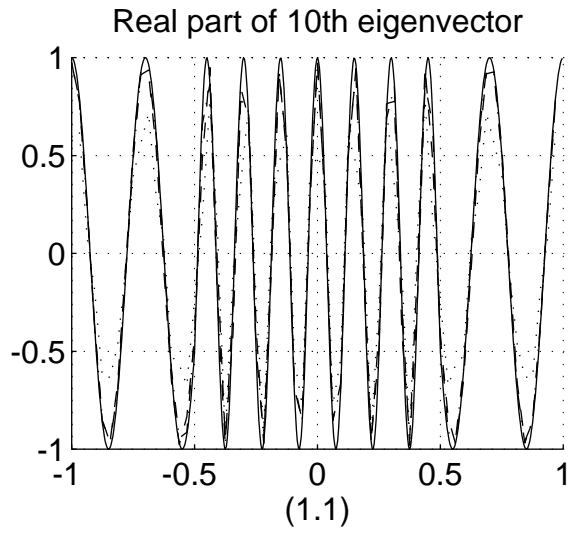


Figure 4: 10th and  $-10$ th eigenfunctions. Solid line represent the analytic eigenfunction; dot line for 8th order finite difference; dash line for the pseudospectral method and dashdot for the pseudospectral method with modified coefficient

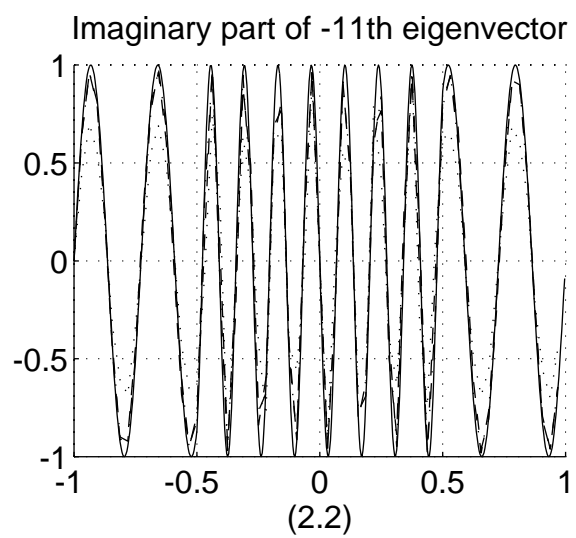
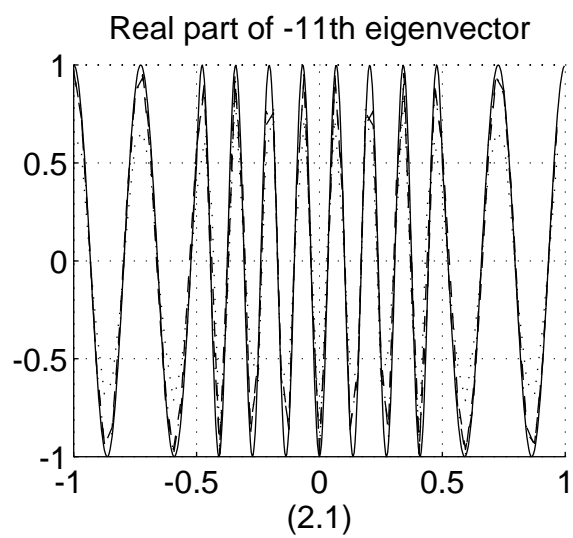
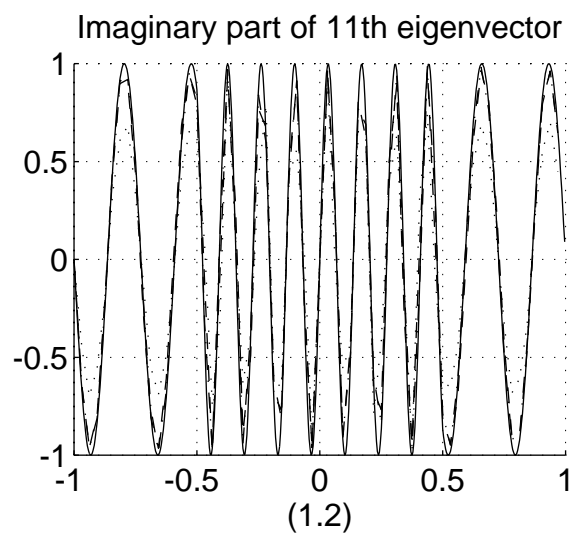
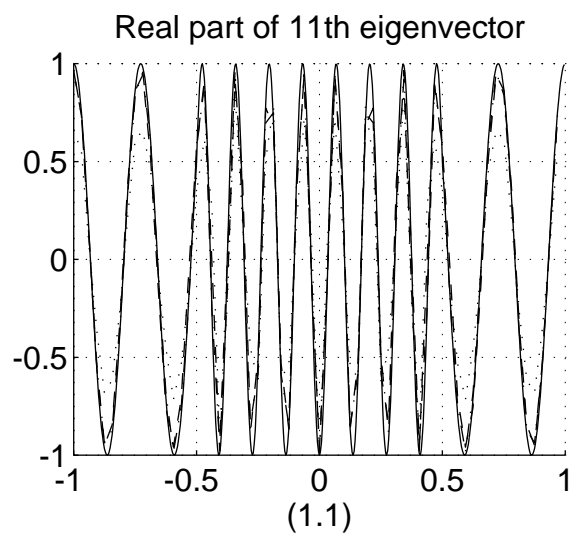


Figure 5: 11th and  $-11$ th eigenfunctions. Solid line represent the analytic eigenfunction; dot line for 8th order finite difference; dash line for the pseudospectral method and dashdot for the pseudospectral method with modified coefficient